

CDF Searches for New Physics with Photons

A. Loginov

Yale University, New Haven, Connecticut 06520

Abstract. We present results of searches for new physics in final states with photons at CDF in approximately 1fb^{-1} of $p\bar{p}$ collisions at 1.96 TeV. We give an overview of the data-driven photon background estimation techniques used for the analyses. We report on a search for diphoton peaks and signature-based searches for $\gamma\gamma + X$, $\ell\gamma + X$ ($X = e, \mu, \cancel{E}_T, \gamma$) and $t\bar{t}\gamma$.

PACS. 13.85.Rm Limits on production of particles – 12.60.Jv Supersymmetric models – 13.85.Qk Inclusive production with identified leptons, photons, or other nonhadronic particles – 14.80.Ly Supersymmetric partners of known particles – 14.80.-j Other particles (including hypothetical)

1 Introduction

A crucial test of the standard model (SM) of particle physics [1] is to measure and understand the properties of the highest momentum-transfer particle collisions, and therefore to study interactions at the shortest distances. The major predictions of the SM for these collisions are the rates for the events of a given type, and their associated kinematic distributions.

Since the predicted high energy behavior of the SM becomes unphysical at an interaction energy on the order of several TeV, new physical phenomena are required. These unknown phenomena may involve new elementary particles, new fundamental forces, and/or a modification of space-time geometry. An anomalous production rate of a combination of the known fundamental particles is likely to be a manifestation of the new phenomena.

The unknown nature of possible new phenomena (Table 1) in the energy range accessible at the Tevatron is the motivation for a “signature-based” search strategy that does not focus on specific models of new physics, but casts a wide net for new phenomena.

In the Tevatron Run I, the rare $ee\gamma\gamma\cancel{E}_T$ candidate event and the measured event rate for the signature $\ell + \gamma + \cancel{E}_T$, which was 2.7 sigma above the SM predictions, sparked signature-based searches in the $\gamma\gamma + X$ [2] and $\ell\gamma + X$ [3] channels. Now in Run II we have performed these searches with an order-of-magnitude larger data set, a higher $p\bar{p}$ collision energy, and the CDF II detector [4]. In these proceedings we report on a search for diphoton peaks and signature-based searches for $\gamma\gamma + X$, $\ell\gamma + X$ ($X = e, \mu, \cancel{E}_T, \gamma$) and $t\bar{t}\gamma$.

2 Techniques

High p_T photons are copiously produced by decays of hadrons in jets resulting from a scattered quark or

SUSY	
$\tilde{\ell} \rightarrow \tilde{\chi}_2^0 + \ell,$	$\gamma\gamma\cancel{E}_T, \ell\gamma\cancel{E}_T, \ell = e \text{ or } \mu$
$\tilde{\chi}_2^0 \rightarrow \gamma\tilde{\chi}_1^0, \tilde{\chi}_1^0 \rightarrow \gamma\tilde{G}$	$\gamma\ell\ell\cancel{E}_T, \gamma\gamma\ell\ell\cancel{E}_T, \ell = e \text{ or } \mu$
Technicolor	
$\omega_T, \rho_T \rightarrow \gamma\pi_T$	$t\bar{t}\gamma, \gamma\gamma\gamma$
$\pi_T \rightarrow \gamma\gamma$	$\ell\ell\gamma\gamma, \ell\ell\gamma\gamma\cancel{E}_T, \ell = e \text{ or } \mu$
Compositeness	
$X^* \rightarrow \gamma X$	$\ell\ell\gamma, \ell\ell\gamma\gamma, \ell = e \text{ or } \mu$
Extra Dimensions (RS)	
$G \rightarrow \gamma\gamma$	$\gamma\gamma$

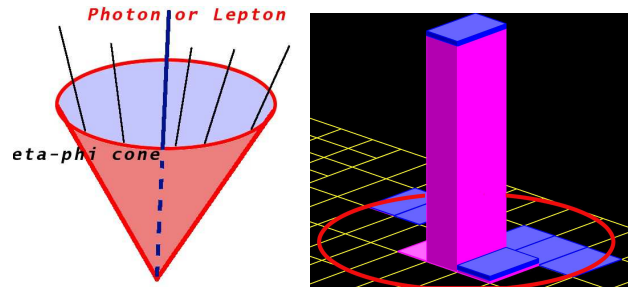
Table 1. Some of the models beyond the SM which predict signatures presented in the talk.

gluon. In particular, mesons such as the π^0 or η decay to photons, which may satisfy the photon selection criteria (see Sec. 2.1). Another important source of non-prompt (“fake”) photons is an electron that undergoes hard bremsstrahlung or whose track is lost due to tracking inefficiency and is misidentified as a photon (see Sec. 2.2).

2.1 Isolation

The backgrounds due to events with jets misidentified as photons or leptons can be estimated by studying the total E_T or p_T of towers or tracks in a cone in $\eta - \varphi$ space of radius $R=0.4$ around the photon cluster or lepton track (see Fig. 2.1). For instance, we estimate the jet-faking-photon background (“ $j \rightarrow \gamma$ ”) for $\ell\ell\gamma$ and $\ell\gamma\cancel{E}_T$ searches [5] by measuring energy in the calorimeter nearby the photon candidate.

Figure 2.2 (a) shows the distribution in the total (electromagnetic plus hadronic) calorimeter energy, E_T^{Iso} , in a cone of radius $R = 0.4$ in $\eta - \varphi$ space around the photon candidate for the $e\gamma\cancel{E}_T$ sample. This distribution is fit to the shape measured for electrons from $Z^0 \rightarrow e^+e^-$ decays plus a linear background.



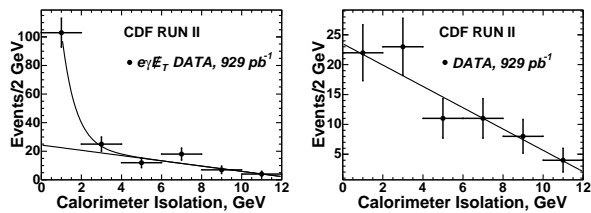
(a) Tracking isolation (b) Calorimeter isolation
Fig. 2.1. Tracking isolation is the $\sum p_T$ of extra tracks around seed track in an $\eta - \varphi$ cone. Calorimeter isolation is the $\sum E_T$ of extra towers around the seed towers in an $\eta - \varphi$ cone. Isolation differs for prompt photons and for ‘fake’ ones.

To verify the linear behavior of the background we select a sample of “fake photons” by requiring the photon candidate to fail the cluster profile criteria. In addition we do not apply the calorimeter and track isolation requirements. The distribution of the total calorimeter energy, E_T^{Iso} , in a cone of radius $R = 0.4$ in $\eta - \varphi$ space around the fake photon candidate is shown in Fig. 2.2 (b).

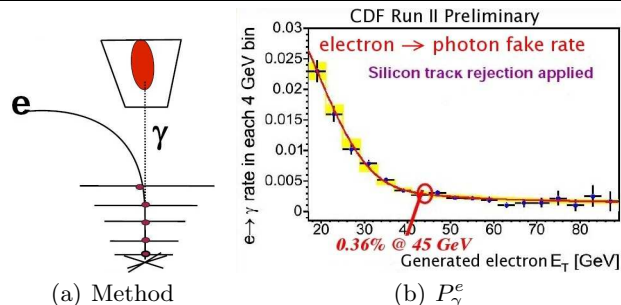
2.2 Phoenix Tracking

If an electron undergoes hard photon bremsstrahlung or no electron track is reconstructed due to the tracking inefficiency, we still can look for track segments in the silicon tracker. To find a segment we seed a “Phoenix” track from an electromagnetic calorimeter cluster and an event vertex and search for hits along the expected arc.

The probability that an electron undergoes hard photon bremsstrahlung and is misidentified as a photon (“ $e \rightarrow \gamma$ ”), P_γ^e , is measured from the control subsample of back-to-back $e\gamma$ events consistent with originating from $Z^0 \rightarrow e^+e^-$ production (Fig. 2.3). The E_T dependence of $P_{e \rightarrow \gamma}$ is obtained from $Z^0 \rightarrow e^+e^-$ simulated sample, and then normalized to data.



(a) Background estimate for $e\gamma E_T$ (b) Calorimeter isolation for “ π^0 ”
Fig. 2.2. The method and data used to estimate the number of background events from jets misidentified as photons for the $e\gamma E_T$ sample (a). The number of events is plotted versus the total (electromagnetic plus hadronic) calorimeter energy, E_T^{Iso} , in a cone in $\eta - \varphi$ space around the photon. This distribution is fit to the shape measured for electrons from $Z^0 \rightarrow e^+e^-$ decays plus a linear background, obtained from a fake photon (“ π^0 ” sample) (b).



(a) Method (b) P_γ^e
Fig. 2.3. The method and data used to estimate the probability that an electron undergoes hard photon bremsstrahlung and is misidentified as a photon, P_γ^e .

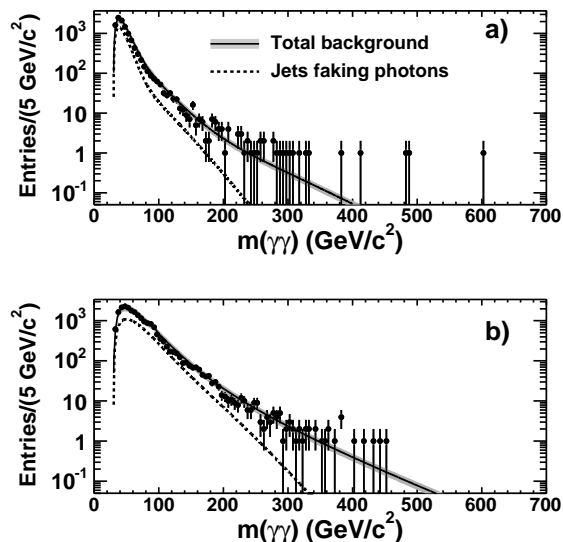


Fig. 3.4. The mass distribution in the CC (a) and CP (b) signal regions with the background overlaid. The points are the data. The dotted line shows the jets which fake photons as predicted from the photon-like jet sample, and the solid line shows this background plus the SM $\gamma\gamma$.

3 Searches

3.1 Search for Diphoton Peaks

One of the signatures for new, heavy particles is a narrow mass resonance decaying to $\gamma\gamma$. This signature could arise from extra spatial dimensions, as in the Randall-Sundrum (RS) model [6]. The spin-2 nature of the graviton, decaying by either s - or p -wave states, favors searching in the $\gamma\gamma$ channel, where the branching ratio is twice that of any single dilepton channel.

In the RS model the widths and masses of the resonances are dependent on the parameter k/\overline{M}_{Pl} , where \overline{M}_{Pl} is the effective four-dimensional (reduced) Planck scale and k is a curvature parameter.

There are two significant components to the diphoton data sample: SM $\gamma\gamma$ production and hadronic jets faking photons. The diphoton mass distribution of the jet background is derived from a sample of photon-like jets obtained by loosening the photon selection criteria, removing events which pass all the signal selection requirements. Figure 3.4 shows the observed mass spectra compared to the predictions.

The values of k must be large enough to be consistent with the apparent weakness of gravity, but small enough to prevent the theory from becoming non-perturbative. Therefore, we examine $0.01 < k/\overline{M}_{Pl} < 0.1$.

To parametrize the background for setting limits, we fit the mass spectra to the combination of a polynomial multiplied by the sum of two exponentials and the expected SM diphoton shape. The 95% confidence-level (C.L.) excluded region in the k/\overline{M}_{Pl} versus graviton-mass plane is shown in Fig. 3.5.

To conclude, we find no evidence of new physics in the diphoton distribution. We evaluate 95% C.L. limits in one model of hypothetical new diphoton production and exclude RS gravitons below masses ranging from $230 \text{ GeV}/c^2$ to $850 \text{ GeV}/c^2$, for a coupling parameter k/\overline{M}_{Pl} of 0.01 to 0.1. This results in a significant improvement, at high mass, over the previous best available limit. Details on this analysis are available in Ref. [7].

3.2 Search for $\gamma\gamma + X$

For the $\gamma\gamma + X$ search we require two photons in the central region with $E_T^\gamma > 13 \text{ GeV}$ in an event. We then perform inclusive searches for additional objects, such as \cancel{E}_T , another γ , e or μ .

The distribution of the \cancel{E}_T in $\gamma\gamma$ events is shown in Fig. 3.6. At low \cancel{E}_T the background is dominated by $\gamma\gamma$, $j\gamma$ and jj ($j \rightarrow \gamma$) events with mismeasured \cancel{E}_T . Intermediate and large \cancel{E}_T regions are populated by $W\gamma \rightarrow e\nu\gamma$ ($e \rightarrow \gamma$) and electromagnetic showers due to cosmic-ray and beam halo muons. The overall agreement between data and the prediction is good. For $\cancel{E}_T > 50 \text{ GeV}$ we find 4 $\gamma\gamma\cancel{E}_T$ events compared to an expectation of 1.6 ± 0.3 events.

For the $\gamma\gamma\gamma$ search we require an additional central photon with $E_T^\gamma > 13 \text{ GeV}$. SM triphoton production is estimated to be 0.80 ± 0.15 events. Fake-photon background is estimated to be 1.4 ± 0.6 events. We find 4 $\gamma\gamma\gamma$ events compared to an expectation of 2.2 ± 0.6 . The distribution for H_T , the sum of the transverse energies of the photons, jets and \cancel{E}_T , is shown in Fig. 3.7. There is good agreement with the expected SM prediction.

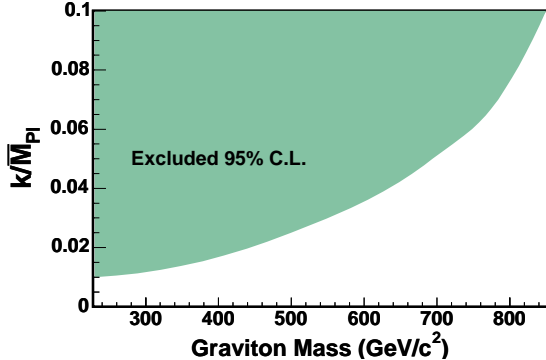


Fig. 3.5. The 95% C.L. excluded region in the plane of k/\overline{M}_{Pl} versus graviton mass.

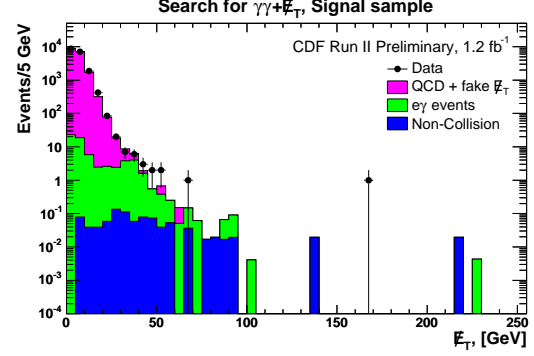


Fig. 3.6. The distribution for the \cancel{E}_T in $\gamma\gamma$ events.

3.3 Search for $l\gamma + X$

To test whether either the $ll\gamma\gamma\cancel{E}_T$ or $l\gamma\cancel{E}_T$ Run I results included new physics effects, we have repeated the $l\gamma + X$ search in 929 pb^{-1} of Run II data. Using the same selection criteria makes this search an *a priori* test, as opposed to the Run I measurement.

We find 163 $l\gamma\cancel{E}_T + X$ events, compared to an expectation of 150.6 ± 13.0 events. The predicted and observed kinematic distributions for the $l\gamma\cancel{E}_T + X$ signature are compared in Fig. 3.8. We observe no $l\gamma\gamma$ or $e\mu\gamma$ events, compared to the expectation of 0.62 ± 0.15 and 1.0 ± 0.3 events, respectively.

We observe 74 $ll\gamma + X$ events, compared to an expectation of 65.1 ± 7.7 events. The predicted and observed kinematic distributions for the \cancel{E}_T in $ll\gamma + X$ events are shown in Fig. 3.9. We find 3 $ll\gamma$ events with $\cancel{E}_T > 25 \text{ GeV}$, compared to an expectation of 0.6 ± 0.1 events (mostly SM $ll\gamma$), corresponding to a likelihood of 2.4%.

We observe no $ll\gamma$ events with multiple photons and so find no events like the $ee\gamma\gamma\cancel{E}_T$ event of Run I.

The $ee\gamma\gamma\cancel{E}_T$ event thus remains a single event selected *a posteriori* as interesting, but whether it was from SM $WW\gamma\gamma$ production, a rare background, or a new physics process, we cannot determine. Details on this analysis are available in Ref. [5].

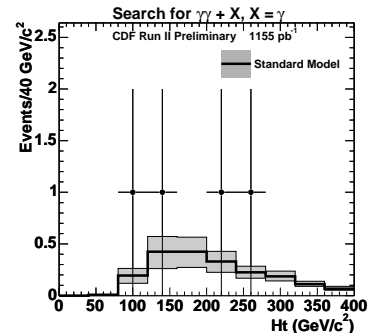


Fig. 3.7. H_T distribution in $\gamma\gamma\gamma$ candidate events, where H_T is the sum of the transverse energies of the photons, jets and \cancel{E}_T .

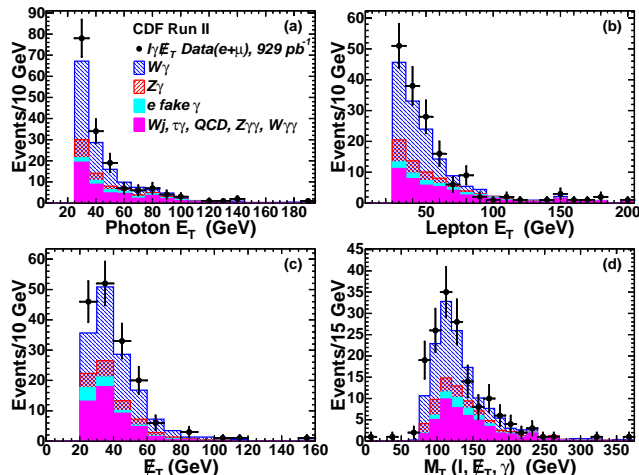


Fig. 3.8. The distributions for events in the $l\gamma E_T$ sample (points) in a) the E_T of the photon; b) the E_T of the lepton (e or μ); c) the missing transverse energy, E_T ; and d) the transverse mass of the $l\gamma E_T$ system. The histograms show the expected SM contributions, including estimated backgrounds from misidentified photons and leptons.

3.4 Search for $t\bar{t}\gamma$

We have searched for the anomalous production of $l\gamma E_T b$ events, such as might be produced in the anomalous production of top quarks, using 929 pb^{-1} of data. SM sources of such events include top quark pairs with an additional photon, $t\bar{t}\gamma$, as well as $W\gamma$ production with b or c quark jets, both of which can result in the signature of a high- p_T lepton, photon, b -tagged jet, and E_T . When one in addition requires large H_T , and ≥ 3 jets, radiative top events dominate the SM prediction. The search is an extension of a investigation of the $l\gamma + X$ signature (Sec. 3.3).

We find 10 $l\gamma E_T b + H_T$ ($H_T > 200 \text{ GeV}$) events (6 for the e channel and 4 for the μ channel) versus an expectation of 7.2 ± 1.0 events (4.9 ± 0.8 and 2.3 ± 0.6 for the e and μ channels, respectively). Figure 3.10 shows the distribution for the total number of jets in $l\gamma E_T b$ events with $H_T > 200 \text{ GeV}$.

For the search for $t\bar{t}\gamma$ events we require $H_T > 200 \text{ GeV}$ along with $N_{jets} \geq 3$. We find 7 such events (4 for the e channel and 3 for the μ channel) versus an expectation of 3.6 ± 0.8 events (2.3 ± 0.6 and 1.3 ± 0.5 for the e and μ channels, respectively).

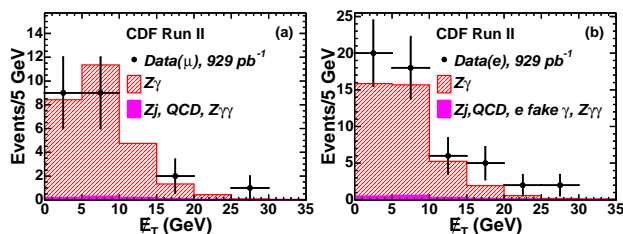


Fig. 3.9. The E_T distributions observed in the inclusive search for a) $\mu\mu\gamma$ events and b) $ee\gamma$ events. The histograms show the expected SM contributions.

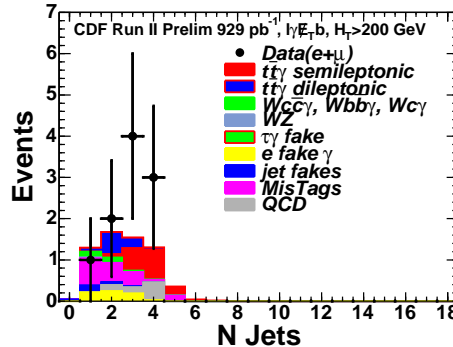


Fig. 3.10. The distribution for the total number of jets in $l\gamma E_T b$ events with $H_T > 200 \text{ GeV}$, where H_T is the total transverse energy, the sum of the transverse energies of the lepton, photon, jets and E_T . For the search for $t\bar{t}\gamma$ events in addition to $H_T > 200 \text{ GeV}$ we also require $N_{jets} \geq 3$. The histogram shows the expected SM contributions.

We find that the numbers of events agree with SM predictions. With enough statistics, in the context of the SM a measurement of the radiative decay of the top quark directly measures the charge of the quark [8]. More generally, events with a top pair with an additional radiated boson, γ , W/Z , or Higgs, both measure the SM couplings and provide windows with small SM cross-sections into which to look for physics processes coupling to the top quark outside the SM [9].

4 Conclusion

The techniques developed and experience gained will be useful for the Tevatron and for the LHC. We find that the number of events in the photon searches agree with the SM predictions. We find no events like the $ee\gamma\gamma E_T$ event of Run I. There are signatures with small number of events expected in datasets analyzed, such as $ll\gamma + E_T$, $\gamma\gamma\gamma$ and $t\bar{t}\gamma$. We look forward to more data in Run II to update and improve the sensitivity of searches for new physics in photon final states.

References

1. S.L. Glashow, Nucl. Phys. **22**, 588 (1961); S. Weinberg, Phys. Rev. Lett. **19**, 1264 (1967); A. Salam, Proc. 8th Nobel Symposium, Stockholm, (1979).
2. F. Abe *et al.* (CDF Collaboration), Phys. Rev. Lett. **81**, 1791 (1998);
3. D. Acosta *et al.* (CDF Collaboration), Phys. Rev. Lett. **89**, 041802 (2002); hep-ex/0202004.
4. T. Aaltonen *et al.* (CDF Collaboration), arXiv:0708.3642;
5. A. Abulencia *et al.* (CDF Collaboration), Phys. Rev. D **75**, 112001 (2007).
6. L. Randall and R. Sundrum, Phys. Rev. Lett **83**, 3370 (1999), hep-ph/9905221.
7. T. Aaltonen *et al.* (CDF Collaboration), arXiv:0707.2294
8. U. Baur, A. Juste, L. H. Orr and D. Rainwater, Phys. Rev. D **71**, 054013 (2005).
9. G. L. Kane and S. Mrenna, Phys. Rev. Lett. **77**, 3502 (1996).